Plant Nano Biology 13 (2025) 100182

Contents lists available at ScienceDirect

Plant Nano Biology

journal homepage: www.journals.elsevier.com/plant-nano-biology

Physiological, metabolic and ionomic responses of *Solanum lycopersicum* plants to Fe_3O_4 and $FePO_4$ nanoparticles

Valerio Petruccelli [a], Emanuele Vaccarella [a], Emma Cocco [a], Francesco Mura [a], Domenico Rosa [c], Alessio Talone [a], Martina Iazzetta [a], Chiara Dal Bosco [b], Alessandra Gentili [b], Luca Di Palma [c], Silvia Canepari [a], Gabriella Pasqua [a], Elisa Brasili [a,*], Lorenzo Massimi [a]

[a] *Department of Environmental Biology, Sapienza-Università di Roma, Piazzale Aldo Moro 5, Roma 00185, Italy*
[b] *Department of Chemistry, Sapienza-Università di Roma, Piazzale Aldo Moro 5, Roma 00185, Italy*
[c] *Department of Chemical Engineering Materials Environment & UdR INSTM, Sapienza-Università di Roma, Via Eudossiana 18, Roma 00184, Italy*

A R T I C L E I N F O

Keywords:
Nanoparticles
Solanum lycopersicum
Ionomics
Metabolic profiling

A B S T R A C T

Fe_3O_4 (NPS-M) and $FePO_4$ (NPS-P) nanoparticles, as representative magnetic materials, have been widely used in the industrial and biomedical fields, although their use in agriculture still needs to be evaluated. The effect of NPS-M and NPS-P in tomato plants was investigated by a combination of phenotypic and metabolic approaches. Tomato plants were grown in soil treated with NPS-M and NPS-P at 0, 5, 50, 100, 500 and 1000 ppm for 8 months. Plant biomass, phenolics and carotenoids in leaves and fruits, soil pH, chlorophyll, and ionome of soil, fruits, roots and leaves, were analysed. NPS-M and NPS-P at higher concentrations increased biomass, total chlorophyll and carotenoid levels in leaves compared to controls. NPS-P caused the major soil acidification, making some nutrients more available to the roots. Although no significant differences were observed in fruit carotenoids, a significant increase in chlorogenic and luteone hexoside levels was observed after NPs treatment at low concentrations compared to controls. Inductively coupled plasma mass spectrometry (ICP-MS) revealed that both NPs compared to EDTA-based chelators resulted in differential element accumulation in roots, leaves/fruits. EDTA-based treatments increased leaf accumulation of Cr, As, K, P, while both NPs increased leaf accumulation of Ca, Co, Sr, Ti, V. Fruit accumulation of Ca, K, and Rb was higher with NPs, while Na, Mg, and P were higher with EDTA-based chelators. The obtained results offer new insights into the response of tomato plants to NPS-M and NPS-P exposure and could be useful for designing alternative strategies to the use of commercial fertilizers.

1. Introduction

With the global population expected to reach 11 billion by 2100, food production must increase by 60–70 % to satisfy the rising demand (Daszkiewicz, 2022). It is well known that traditional methods like pesticides, chemical fertilizers, and genetically modified seeds are unsustainable and excessive use of chemical fertilizers degrades soil, decreases food quality, and causes environmental issues, including leaching, mineralization, and widespread ecosystem impacts (Gamage et al., 2024). This necessitates advancements in farming and agriculture. Plants require external micronutrients and macronutrients for optimal growth (Ahmed et al., 2024). Amont them, iron (Fe) and phosphorus (P) a micronutrient and a macronutrient, respectively, are crucial but their low bioavailability significantly hinders crop productivity (Barber, 1995). Fertilizers addressing Fe and P deficiencies have notable environmental and economic consequences due to high Fe chelate leachability (Priya et al., 2024) and low P fertilizer nutrient use efficiency (NUE), typically 10–20 % (Baligar et al., 2001). Nonetheless, fertilizers are essential, as Fe and P deficiencies affect nearly 30 % and 65 % of arable land, respectively (Priya et al., 2024). Fe deficiency is a global agricultural issue, despite high total soil Fe, due to limited bioavailability in alkaline soils (Zuo et al., 2011). This nutritional disorder reduces vegetative growth, yield, and quality in agricultural crops (Abadía et al., 2011). Fe is vital for metabolic processes, including mitochondrial respiration, fatty acid and protein synthesis, and photosynthesis (Kobayashi et al., 2019). It is also crucial for CO2 fixation and biomass production (Zhang et al., 2019). Fe-deficient plants show reduced photosynthetic activity and yellowing/interveinal chlorosis in young

* Corresponding author.
E-mail address: elisa.brasili@uniroma1.it (E. Brasili).

https://doi.org/10.1016/j.plana.2025.100182
Received 3 July 2025; Received in revised form 26 July 2025; Accepted 7 August 2025
Available online 8 August 2025

leaves. Foliar Fe treatments are short-lived, and Fe chlorosis is often managed by increasing soil Fe availability, such as with Fe ethylenediaminetetraacetic acid (EDTA-Fe) (Sun et al., 2022, 2023). However, EDTA-Fe can release pollutants upon degradation, highlighting the need for sustainable Fe supply and chlorosis treatment methods. P is a macronutrient with key roles in plant biochemistry, serving as a structural element of nucleic acids and phospholipids, and involved in energy transfer, respiration, and photosynthesis (Hawkesford et al., 2012). P-deficiency symptoms include reduced leaf expansion, increased chlorophyll content, and a decreased shoot/root ratio due to inhibited shoot growth (Hawkesford et al., 2012).

In the last decade, nanotechnology has offered a promising solution for sustainable agriculture and enhanced crop production through targeted delivery of agricultural products, minimizing waste and environmental impact (Chhipa, 2017; Mariyam et al., 2023; Goyal et al., 2023). Overall, nanotechnology can significantly enhance agricultural practices, boosting food production, improving food safety, and fostering a more sustainable food system. Operating at the ultra-small scale (<100 nm), nanoparticles (NPs) can improve crop yields, combat diseases, and promote sustainability (Arora et al., 2024). In this context, nano-fertilizers supply nutrients directly to plant roots, improving uptake and reducing waste, leading to healthier plants and higher yields. Nanotech-based fertilizers can be designed for slow nutrient release, ensuring optimal uptake and less frequent applications. Nanofertilizers and bionanofertilizers are key nano-based products for sustainable agriculture, providing efficient, targeted nutrient delivery (Sun et al., 2022). In this context, nanomaterials enhance fertilizer use efficiency, either as fertilizers or carriers (Wu et al., 2022). They are effective because they can cross plant barriers like cell walls and epidermis, traversing cell membranes and organelles to reach various plant parts via vasculature under specific conditions (Wu et al., 2022). Understanding complex NP-plant interactions is crucial for field-scale nanotechnology applications in agriculture. Magnetite (Fe3O4) and iron phosphate (FePO4) NPs have successfully improved P and Fe availability, promoted photosynthesis, and enhanced salt and disease resistance (Sega et al., 2019, Feng et al., 2022). Nano-sized magnetite particles, with exceptional physical, chemical, and optical properties, are a popular choice for current NP research. However, the precise mechanisms by which these advanced fertilizers support sustainable agriculture—by boosting crop yields, enhancing soil quality, and reducing environmental harm—are not fully understood. Recent metabolomics studies suggest that nanoparticles affect the biosynthesis of bioactive compounds, such as phenolic compounds and carotenoids, by modulating reactive nitrogen/oxygen species, gene expression, and signalling pathways (Cantu et al., 2022; Selvakesavan et al., 2023).

Over the past decades, ionomics, the study of metal and metalloid accumulation by living organisms, has gained popularity for assessing plant nutrient content related to stress factors. Ionomics helps study variability in plant nutrient content due to exposure to varying concentrations of potentially toxic elements (Singh et al., 2013; Watanabe et al., 2016). While primarily applied to toxic heavy metals (As, Cd, Pb), there's a recent increase in environmental concentrations of metals like bismuth (Bi) and lithium (Li), used to replace toxic heavy metals (Zacchini et al., 2023; Iannilli et al., 2024; Iannilli et al., 2025). Several studies have applied ionomics to *S. lycopersicum* under various stresses (Sánchez-Rodríguez et al., 2010; Xiao et al., 2022) and to study nutrient supply to edible plant parts (Watanabe et al., 2016). This study is the first to apply an ionomic approach to simultaneously evaluate the uptake and translocation of numerous elements in different *S. lycopersicum* tissues grown with various chelators, and to assess their potential effects on the plant's metabolic profile. The main objective was to comprehensively assess the effect of FePO4 (NPs P) and Fe3O4 (NPs M) NP application, compared to conventional chelators like EDTA and EDTA-Fe, on *S. lycopersicum* plants. We explored the metabolic profiling (phenolics and carotenoids by HPLC-MS) and the ionome (by ICP-MS) to assess dissolution, bioaccumulation, and translocation dynamics of 30 elements in *S. lycopersicum* plants exposed (or not, as control) to culture media enriched with 5, 50, 100, 500, and 1000 mg Kg-1 of EDTA, EDTA-Fe, magnetite NPs (NPS-M), and iron phosphate NPs (NPS-P) at different growth stages.

2. Material and methods

2.1. Preparation of nanoparticles

In order to synthesize $FePO_4$ Nanoparticles (NPs-P), 50 mL of a 2 M $FeSO_4$ (Carlo Erba) solution was added to 50 mL of a 2 M H_3PO_4 (Carlo Erba) solution and stirred for 30 min. Subsequently, 50 mL of a 1.2 M H_2O_2 (Honeywell) solution was added dropwise. Under continuous stirring and pH monitoring, a 2 M NH_3 (Sigma-Aldrich) solution was then added dropwise. The formation of a white precipitate, identified as $FePO_4$ nanoparticles, was observed as the pH was adjusted to 2. This pH value was maintained to prevent the formation of undesired iron oxides or hydroxides. The suspension was allowed to settle, and the supernatant was repeatedly removed and replaced with demineralized water until the pH reached 5 (operating pH). This washing process removed reaction residues without drying the solid, thus avoiding potential nanoparticle aggregation (Hsieh et al., 2012). With the aim of synthesizing Magnetite (Fe_3O_4) Nanoparticles (Nps-M), 4.43 g of ferric chloride hexahydrate ($FeCl_3 \cdot 6\ H_2O$, Honeywell) and 2.10 g of ferrous chloride ($FeCl_2$, Honeywell) were dissolved in 150 mL of a 0.2 M hydrochloric acid (HCl, Carlo Erba) solution under constant stirring for 2 h at room temperature to ensure complete solubilization of the iron salts. Subsequently, 50 mL of a 3 M sodium hydroxide (NaOH) solution was added dropwise, immediately forming a brown precipitate. The suspension was kept under constant stirring for 3 h. The solid was then filtered and washed with demineralized water to remove residual reaction species (Cl^-, Na^+, and OH^-) until neutral pH (7) was achieved (Rosa et al., 2023). Finally, the product was dried in an oven at 60 °C overnight and ground using a mortar.

2.2. Chemical characterization of nanoparticles

The morphology of the materials was examined using scanning electron microscopy (SEM). SEM images were recorded with a high-resolution field emission scanning electron microscope (HR-FESEM, AURIGA Zeiss) at 15 kV.

2.3. Plant growth conditions and measurements

Seeds from *S. lycopersicum* F1 "zucchero" were germinated in the dark in a climate room at 24/26 °C on Petri dishes hydrated with 2 mL of a double-distilled water solution at pH 5.0, containing Hoagland salts (H2395; Sigma-Aldrich). After a week, germinated seeds were transferred to pots containing universal soil (COMPO SANA®) and potted seedlings (one per pot) were grown in growth chambers at 24/26 °C and humidity controlled with a 16/8 h photoperiod for 8 months. Three pot sizes were used: 1) pots of 0.10 L were used for plant germination up to 15 days after germination; 2) pots of 0.50 L were used from 15 days to 2 months after germination; 3) pots of 1.7 L were used from two months to eight months after germination. A total of 80 plants were used, i.e. 5 replicates for each concentration (5, 50, 100, 500 and 1000 mg/L) of each treatment (EDTA-Fe, NPs-M and NPs-P) and 5 replicates for the control treated with water. The tomato plants were treated once a week for 8 months with aqueous solutions containing different concentrations of NPs and EDTA-Fe or EDTA, and irrigated weekly with 250 mL of water per pot. The measurement of soil pH was carried out using the Hanna pH meter (Edge HI2002–01 series). The pH was measured at 1, 3, 5, 7 and 8 months of the plant life cycle, for each replicate of each concentration of NPS-M and NPS-P treatment to verify differences compared to control samples. Fresh weight (FW) and dry weight (DW) of total biomass for each replicate were measured for each plant treatment.

To obtain the dry weight, the biomass was dried in an oven at a temperature of 60 °C for 48 h. The fruits were collected at the ripening stage, counted and weighed.

2.4. Determination of chlorophyll and carotenoid content in leaves

Chlorophylls and carotenoids were extracted from the leaves of *S. lycopersicum* and examined at four times: 1, 3, 5 and 7 months after germination. For the extraction, methanol (96 % v/v) was added to the leaves in a ratio of 1:50 (1.0 g of plant matrix/ 50 mL of MetOH). The samples were extracted in the dark for 72 h at a temperature of 4 °C. Subsequently, the supernatant was recovered and analyzed with the Shimadzu UV-1280 spectrophotometer. Chlorophylls a and b were analyzed at a wavelength of 666 nm and 653 nm respectively, while the reading of total carotenoids was carried out at a wavelength of 470 nm (Dere et al., 1998). The values obtained from the readings were used for subsequent quantification according to the formulas of Lichtenthaler and Wellburn (1983):

$Ca = (15.65 \times \lambda 666) - (7.340 \times \lambda 653)$

$Cb = (27.05 \times \lambda 653) - (11.21 \times \lambda 666)$

$Cc = (1000 \times \lambda 470) - (2.860 \times Ca - 129.2 \times Cb\ 245)$

Where: Ca = chlorophyll a; Cb = chlorophyll *b*; Cc = total carotenoids; λ = wavelength

2.5. Analysis of phenolic compounds in tomato fruits by HPLC-DAD-MS

The analysis of phenolic compounds was performed according to the protocol of Ribas-Agusti (2012) with some modifications. For the LC-MS analysis of carotenoids, fruits collected at the same stage of ripening were considered.

All solvents and standards were purchased from Sigma Aldrich (St. Louis, MO, USA) except MS ultrapure water that was produced by a Milli-Q Plus apparatus (Millipore, Bedford, MA, USA) and potassium hydroxide (KOH) and magnesium carbonate were obtained from Carlo Erba (Milan, Italy). Tomato fruits were lyophilized and finely ground into powder using a laboratory mixer. A 200 mg aliquot of the powdered sample was extracted with 2 mL of methanol and sonicated for 30 min to enhance compound solubilization. The samples were subsequently incubated at 4 °C overnight under dark conditions to prevent phenolic degradation. Following incubation, the extracts were centrifuged on an Itettich Zentrifugen centrifuge (Germany) at 10.000 g for 20 min at 4 °C. The resulting supernatant was carefully filtered through 0.22 µm membrane filters and stock at −80 °C prior to HPLC-DAD-MS analysis. To quantify the target compounds, calibration curves were constructed for chlorogenic acid, ferulic acid, rutin, luteolin, and naringenin chalcone. Chlorogenic acid, rutin, and naringenin chalcone were used as external standards, enabling direct quantification of these compounds in the samples through their respective calibration curves. Ferulic acid and luteolin, instead, were employed as internal standards to facilitate the relative quantification of caffeic acid hexoside and luteone hexoside. For all compounds, preparative dilutions were performed starting from a 1 mg/mL stock solution to obtain working solutions with concentrations of 100, 50, 20, 10, 5, 2, and 1 µg/mL. Analyses were performed with an HPLC system consisting of a 1260 Infinity II flexible pump, a 1260 Infinity II autosampler, and an HS1260 Infinity II diode array detector set at lambda of 278 nm (Agilent, Santa Clara, CA, USA). An InfinityLab Poroshell 120 EC-C18 column (3.0 mm × 150 mm, 2.7 µm) (Agilent, Santa Clara, CA, USA) was used as a stationary phase at a temperature of 35 °C and 5 µl injection volume. MS setup: Ion source ESI, Analyzer: Agilent Infinity Lab LC/MSD Series and 6100 Series LC/MS Single quadrupole (SQ)setting: negative Full scan 50–1000 *m/z*, Fragmentor 100, Gas T = 325 °C, Gas flow 13 L/min), Nebulizer 55 psi, Capillary Voltage 3500 V. The mobile phases were as follows: A (Milli Q water 0.05 % Formic acid) and B (Acetonitrile 0.05 % Formic acid). The HPLC gradient with a flow tare of 0.8 mL/min, begins with 5 % B, at 3.00 min it increases to 8 % B, at 9.00 min to 10 % B, and remains constant at 16.00 min. At 22.00 min, it shifts to 20 % B, at 23.00 min to 23 % B, at 37.00 min to 30 % B, and at 47.00 min to 40 % B. At 48.00 min, it changes to 100 % B, which is used for washing the column, and remains constant at 58.00 min. Finally, at 59.00 min, it returns to 5 % B to recondition the column until 69.00 min.

2.6. Analysis of carotenoids in tomato fruits by LC-MS

The extraction of carotenoids from tomato fruits was conducted as previously reported by Brasili et al. (2020). Briefly, 1 g of lyophilized sample was mixed to 6 mL of ethanol containing 0.1 % butylated hydroxytoluene (BHT, w/v) and 1 mL of 50 % potassium hydroxide (KOH, w/v). The mixture was incubated overnight at 25 °C under constant agitation in dark conditions to prevent carotenoid degradation. Subsequently, a volume of 3 mL of Milli-Q water was added to the mixture. The extraction process involved two sequential steps where 12 mL of hexane containing 0.1 % BHT (w/v) was added, followed by 5 min of gentle agitation and 5 min of vortexing. The samples were then centrifuged at 6000 rpm for 10 min at 4 °C, and the hexane phase (upper layer) was collected from both steps into a single tube. Further details are reported in Supplementary Material (Section Material and Methods).

2.7. ICP-MS Chemical analysis

The samples were lyophilized for 48 h and then the dry weight (DW) was recorded. Afterward, 100 mg (DW) of each sample (two replicate per sample) underwent microwave-assisted acid digestion (Ethos Touch Control system with a Q20 rotor; Milestone, Bergamo, Italy) at 180 °C for 30 min, employing a mixture of HNO_3/H_2O_2 (nitric acid 65 %, Carlo Erba, Rome, Italy; hydrogen peroxide Suprapur, Merck, Billerica, MA, USA) in a 2:1 (v/v) ratio. Subsequently, the digested solution was diluted 1:1000 with deionized water and filtered through cellulose nitrate syringe filters (GVS Filter Technology, Morecambe, England, UK) with a diameter of 25 mm and a pore size of 0.45 µm. The concentrations of 30 macro-, micro-, and trace elements (Al, As, Be, Bi, Ca, Cd, Ce, Co, Cr, Fe, K, La, Li, Mg, Mn, Mo, Na, Nb, Ni, P, Pb, Rb, Sr, Ti, Tl, U, V, W, Zn, Zr) in each sample were determined using an inductively coupled plasma mass spectrometer (ICP-MS; PlasmaQuant MS Q, Analitik Jena, Jena, Germany) equipped with a glass nebulizer (0.4 mL min^{-1}; Analytik Jena AG, Jena, Germany). Three replicates were performed for each measurement, showing standard deviations < 5 %. The calibration curve was generated by serially diluting 1000 ± 2 mg L^{-1} multi-standard stock solutions (Merck Millipore Ltd., Billerica, MA, USA). Two internal standards, yttrium and rhodium were used for all measurements to control nebulizer efficiency. The limit of detection (LOD) of each element, determined as the mean plus three times the standard deviation (SD) of five replicate blank determinations, is reported in supplementary materials (Table S1, S2, S3, and S4) along with the element concentrations of the samples collected at the latest growth stage (T4). Element concentration (mg/Kg) was calculated dividing the content of each element by the DW of each sample. The instrumental conditions and performance of the method were according to Canepari et al., (2009).

2.8. Statistical analysis

Data were statistically analyzed using Sigma Plot (version 12.0, Sysstat Sofware, Inc., USA). The results were reported as mean ± standard deviations. Differences between groups were tested using One-way Anova followed by Holm-Sidak Test for plant biomass, chlorophyll, pH, phenolic acids and carotenoids levels. Significance was set at $p < 0.05$. For ICP-MS, a total of 6300 data were obtained, containing 30 element concentrations in 210 biological samples, including 84 soil and 84 root samples (20 samples per treatment plus 1 control sample for each of the four growth stages) and 21 leaf and 21 fruit samples for the last growth stage (T4). An explorative PCA was applied to the whole dataset, and to the leaf and fruit samples separately, using the software CAT

(Chemiometric Agil Tool, R. Leardi, C. Melzi, G. Polotti, CAT) to investigate relationships between the element concentrations for each treatment in the different plant tissues at the fourth growth stages. The influence of the elements bioaccumulated on the content of phenolic compounds and carotenoids in tomato fruits was also explored by PCA.

3. Results

3.1. Chemical characterization of nanoparticles

The SEM investigation of NPS-M and NPS-P is shown in Figs. 1**a** and 1**b**. Both types of nanoparticles exhibited a relatively heterogeneous distribution. NPS-M had an average size of approximately 90 nm, characterized by jagged edges and anisotropic crystalline structures. In contrast, the NPS-P appeared as spherical particles with an average size of approximately 100 nm, showing an isotropic size distribution.

3.2. Effect of NPS-M and NPS-P on plant biomass, total chlorophyll and carotenoids, soil pH, and fruits

Table S1a and b report the fresh weight (FW) and dried weights (DW) of the plant biomass. Both NPS-M and NPS-P treatments significantly increased plant FW and DW across all concentrations compared to controls. Specifically, NPS-P-100 resulted in the highest FW, while NPS-P-5 led to the lowest FW. For DW, NPS-M-1000 achieved the highest weight, with NPS-P-5 being the lowest. Notably, NPS-P at 100 ppm led to a significantly greater increase in both FW and DW compared to NPS-M at the same concentration. While a directly proportional relationship between weight gain and nanoparticle concentration was not consistently observed, plants treated with NPS-M reached their maximum weight at 1000 ppm, with no significant differences among other NPS-M concentrations. Conversely, NPS-P treatments achieved their peak weight at 100 ppm, showing significant differences in FW and DW at both lower and higher concentrations compared to 100 ppm.

In contrast, EDTA and EDTA-Fe treatments at 500 and 1000 mg/L dramatically reduced plant biomass compared to the control. Although a slight increase in FW and DW was observed in plants treated with EDTA-Fe over those treated with EDTA, the severe toxicity of EDTA was evident at 500 and 1000 mg/L, regardless of the presence of iron. Table S2, shows fruit weights. No significant differences were observed in fruit weight between NPS-M or NPS-P treatments and the control across all concentrations. However, EDTA-Fe at 100 mg/L significantly reduced fruit weight compared to the control. In addition, plants treated with EDTA and EDTA-Fe at 500 and 1000 mg/L did not reach the ripening stage, further indicating their toxicity.

The Table S3 illustrates soil pH values over an 8-months period following the treatment with NPS-M, NPS-P and EDTA-Fe at different concentrations. At 1 month, all groups exhibit a near-neutral pH. The most significant pH variability occurred between 1 and 3 months of plant growth, depending on the NPS treatment. Specifically, increasing NPS-M concentrations (50, 100, 500, and 1000 mg/L) consistently reduced soil pH over time compared to control and EDTA-Fe groups. A similar acidification trend was observed with NPS-P at 50, 100, 500, and 1000 mg/L. Interestingly, NPS-M treatments resulted in significantly higher pH values than NPS-P at the same concentrations (NPS-50 mg/L). At 3 months, NPS-M and NPS-P at 1000 mg/L caused the greatest soil acidification, reaching pH values of 5.51 and 5.37, respectively. Interestingly, at 5 months, significant differences were observed between NPS-M and NPS-P at the same concentration, with NPS-P treatments maintaining lower soil pH compared to NPS-M at 5, 100, 500 and 1000 mg/L. This trend persisted at 7 and 8 months, where soil pH remained stable, but values were consistently higher in NPS-M treated soil compared to NPS-P.

The dynamics of total chlorophyll and carotenoid content in plant leaves under various treatments over time is shown in Figure S1. NPS-M and NPS-P treatments consistently enhanced total chlorophyll content compared to the water control at all time points (1, 3, 5, and 7 months). Conversely, EDTA-Fe at 500 and 1000 mg/L drastically reduced total chlorophyll levels, by 53.94 % and 65.45 % respectively compared to the control after 5 months, indicating severe phytotoxicity. Notably, NPS-P at 500 and 1000 mg/L was more effective than NPS-M at equivalent concentrations in increasing chlorophyll.

The total carotenoid content in leaves followed a similar trend to chlorophyll levels. Within 1 month, NPS-M (at all concentrations except 1000 mg/L) and NPS-P (at 5, 50, and 500 mg/L) increased total carotenoids compared to controls. In contrast, EDTA-Fe at 500 and 1000 mg/L significantly reduced carotenoid levels by 14.21 % and 14.98 %, respectively. By 7 months, NPS-P at 1000 mg/L outperformed NPS-M in increasing carotenoid content.

3.3. Impact of NPS-M and NPS-P on phenolic compounds and carotenoids

The identification of chlorogenic acid, rutin and naringenine chalcone was confirmed by comparison with their standard, while the identification of caffeic acid hexoside and luteolin hexoside was confirmed through MS and UV spectra, which revealed the $[M-H]^-$ ion peak and the corresponding neutral loss of 162 Da, characteristic of the respective aglycone molecules (Table S4).

The levels of chlorogenic acid significantly increased in tomato fruits after treatment with all EDTA concentrations and NPS-M at 50 mg/L compared to control samples. EDTA at 500 mg/L significantly increased chlorogenic acid compared to NPS-M and NPS-P at the same concentration. Among NPs, the treatments with NPS-M at 50 mg/L and NPS-P at 5 mg/L were the most efficient in determining an increase in the levels of chlorogenic acid. NPS-M at 50 mg/L also increased the level of luteone hexoside compared to controls. No significant differences were observed in other identified phenolic compounds (Fig. 2).

Evaluation of the effect of treatments was performed considering the most abundant carotenoids, which are listed in Table S5. No significant variations were observed among group treatments.

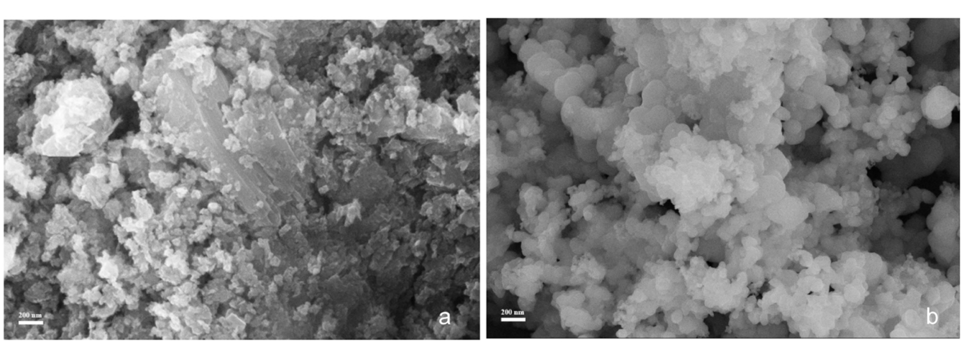

Fig. 1. SEM images of a) Fe_3O_4 and b) $FePO_4$ NPs.

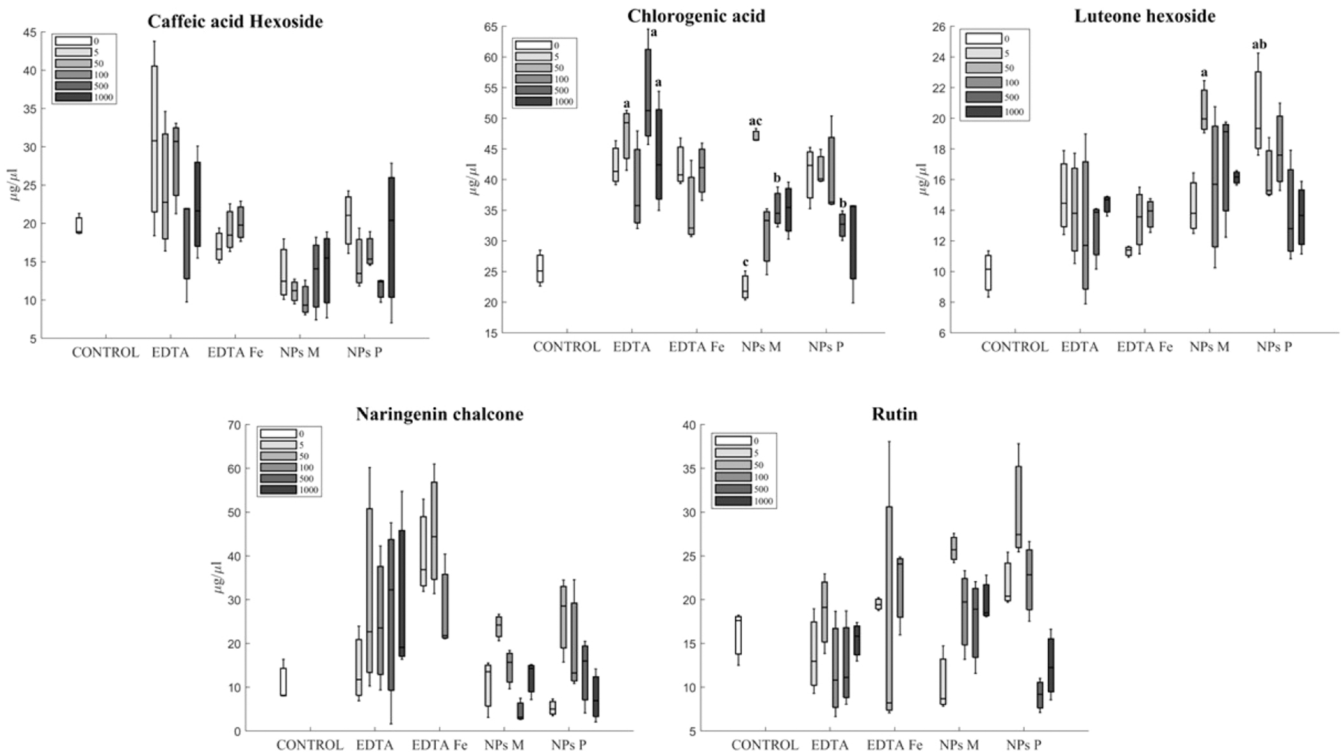

Fig. 2. Phenolic acids in tomato fruits treated with water (control), EDTA, EDTA-Fe, NPS-M and NPS-P. Within each box, horizontal black lines denote median values; boxes extend from the 25th to the 75th percentile of each group's distribution of values; vertical extending lines denote adjacent values (i.e., the most extreme values within 1.5 interquartile range of the 25th and 75th percentile of each group); Different letters represent significant differences at Mann-Whitney *U* test. Letter a: EDTA 500, EDTA 50, EDTA 1000, NPS-M 50 vs Control; b: EDTA 500 vs NPS-P and NPS-M 500; c: NPM 50, EDTA-Fe 5, EDTA 5, NPS-P 5 vs NPM 5. A *p-value* < 0.05 was considered statistically significant.

3.4. Impact of NPS-M and NPSP on ionome of soil, leaves and fruits in tomato plants

The results obtained from elemental analysis of *S. lycopersicum* plants showed large differences in the four growth stages in both soil and root samples **(**Fig. 3**)**. On the other hand, the difference among treatments was rather small and mainly related to the use of EDTA- or NPs-based chelators. As can be seen from Tables S6-S9**,** showing element concentrations in soil, root, leaf, and fruit samples at T4, crustal elements such as Bi, Ba, Co, Cr, and Zr showed higher concentrations in the soil samples and were not accumulated in the plant root system in any of the treatments. In contrast, Mo, K, Mn, As Rb, Mg, and Zn were accumulated in the roots. In both Tables S6-S9 and Fig. 3, (showing Mg concentrations in all analyzed samples at the fourth growth stages), we can observed that these elements were accumulated in roots at T1 (Fig. 3a) and T2 (Fig. 3b), while from T3 (Fig. 3c), their concentrations in roots decreased, presumably for their translocation in leaves or fruits, as can be seen for Mg at T4 (Fig. 3d). At T1, nutrients (such as Mg), as well as potentially toxic elements, increased in concentration in the root system of *S. lycopersicum* plants as the concentration of EDTA and EDTA-Fe increased (5–500 mg/L for EDTA, and 5–1000 mg/L for EDTA-Fe), likely because EDTA treatments enhanced the solubility of the elements and thus their bioavailability in the growth medium. In particular, concentrations significantly increased compared to the control from 50 to 1000 mg/L (*p-value* < 0.05). This behaviour was less pronounced for treatments in which increasing concentrations (5–1000 mg/L) of NPS-M and NPS-P were used, which thus appeared to influence element bioavailability less. In addition, it can be seen that at growth stages T2 and T3 (Fig. 3b and c), the accumulation of essential nutrients (such as Mg) decreased dramatically, as they were predominantly uptake at T1 and less available in the soil, while nonessential nutrients and potentially toxic elements, although present in lower concentrations in the growing medium, continued to be accumulated by the root system (Table S7). Furthermore, Fig. 3d and Table S9, show that at T4, Mg (and most of the macro-nutrients) were translocated into the leaves and fruits while the potentially toxic elements and nonessential nutrients did not undergo substantial translocation into the aerial organs and remained mainly accumulated in the root system. In particular, Mg was translocated and accumulated in the leaf apparatus in concentrations about three times higher than in the roots (Fig. 3d).

The results obtained from the explorative PCA are shown in Figure S2 and Fig. 4. The variance explained by the first 4 components explored is: 57.1 %, 12.6 %, 9.3 % and 6.4 %. The first component shows the main variability (57.1 %) between the data, which is related to the different element concentrations in the two matrices considered (plant and soil samples). Excluding PC1 and exploring PC2/PC3 (Figure S2a and S2b) allows investigating the relationships between the concentrations of the 30 elements (Figure S2b) in the different plant samples (root, leaf, and fruit samples) between treatments (variance explained by PC2) at different growth stages (variance explained by PC3).

Most of the elements (Figure S2b), such as K, Mn, Rb, and P were accumulated in the root system as early as T1, nonessential nutrients and toxic elements (group A, Figure S2b) like As, Cd, Sr, W, and Zn were mainly accumulated in the roots at T2, when macro-nutrients availability in soil was reduced. On the other hand, Bi, Ce, Co, Li, Ni, and U, which were not translocated and accumulated in the plant tissues and remained at the highest concentrations in the soil samples (group C, Figure S2b), are clustered in the center of the loading plot due to their low variability in the plant samples. Exploring PC3/PC4 (Fig. 4a and b) it is possible to investigate the variability of element concentrations (group C, Fig. 4b) in the plant samples due to the different translocation and accumulation of Ca, Li, Mg, Mo and Sr in the leaf samples (marked in red in Fig. 4a) compared to As, Cd, K, Mn, Na, Rb, P, W and Zn (groups A

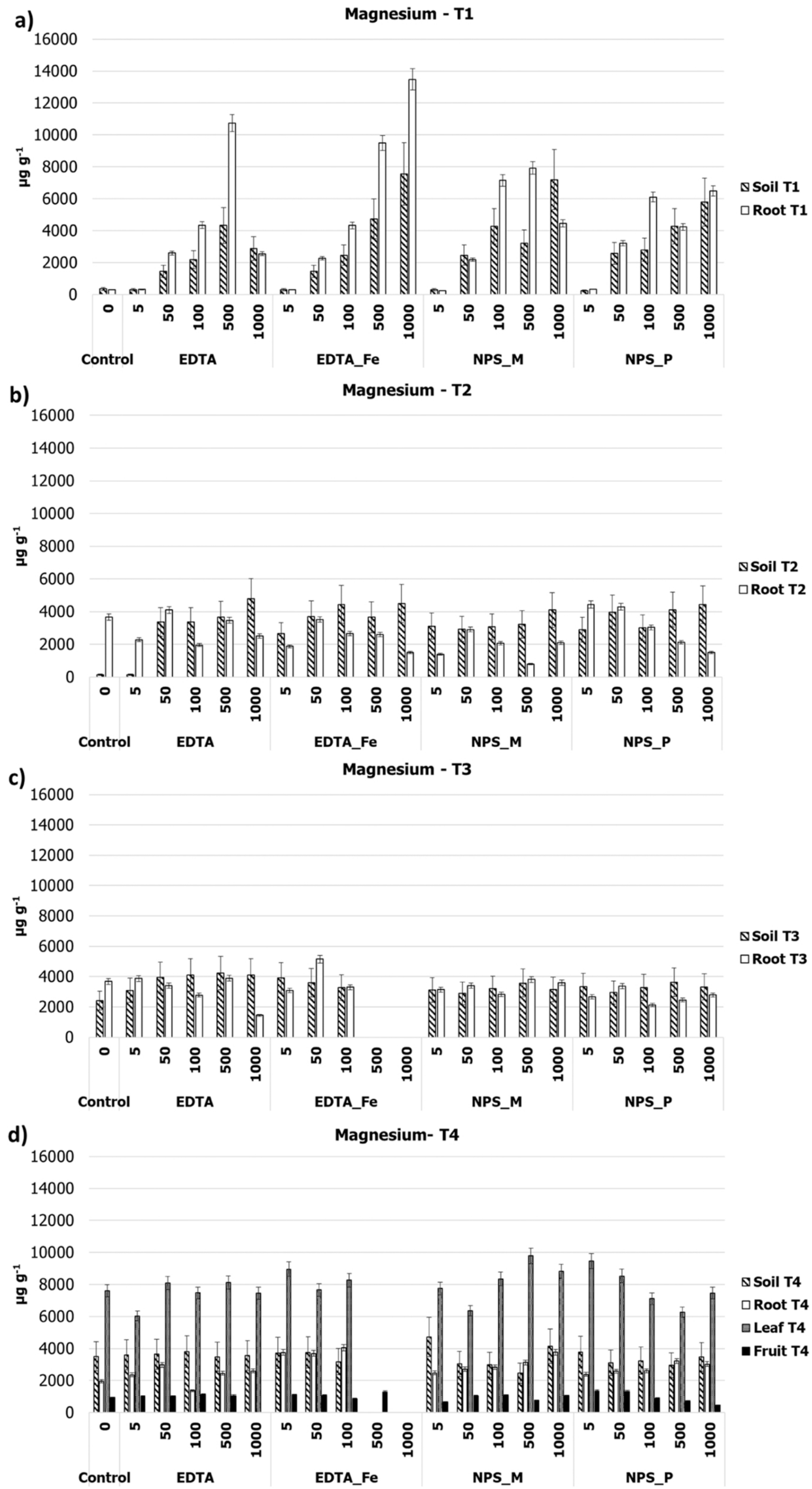

Fig. 3. Mg concentrations in soil, root, leaf and fruits at all experimental times (T1-T4).

and B, Fig. 4b), which instead were mainly accumulated in the root system and/or translocated in the fruits. In fact, among these, the nutrients K, Mn, Rb, and P (group B, Fig. 4b) were at the highest concentrations in the root samples at T1 and in the fruit samples (marked in black in Fig. 4a) at T4.

To understand the effects of the different treatments on element translocation in plant leaves and fruitsand on variations in phenolic compounds and carotenoid concentrations in tomato fruits, an explorative PCA was performed on the data obtained on leaf (Figure S3a and S3b) and fruit (Fig. 5a and b) samples at the last growth stage (T4). As

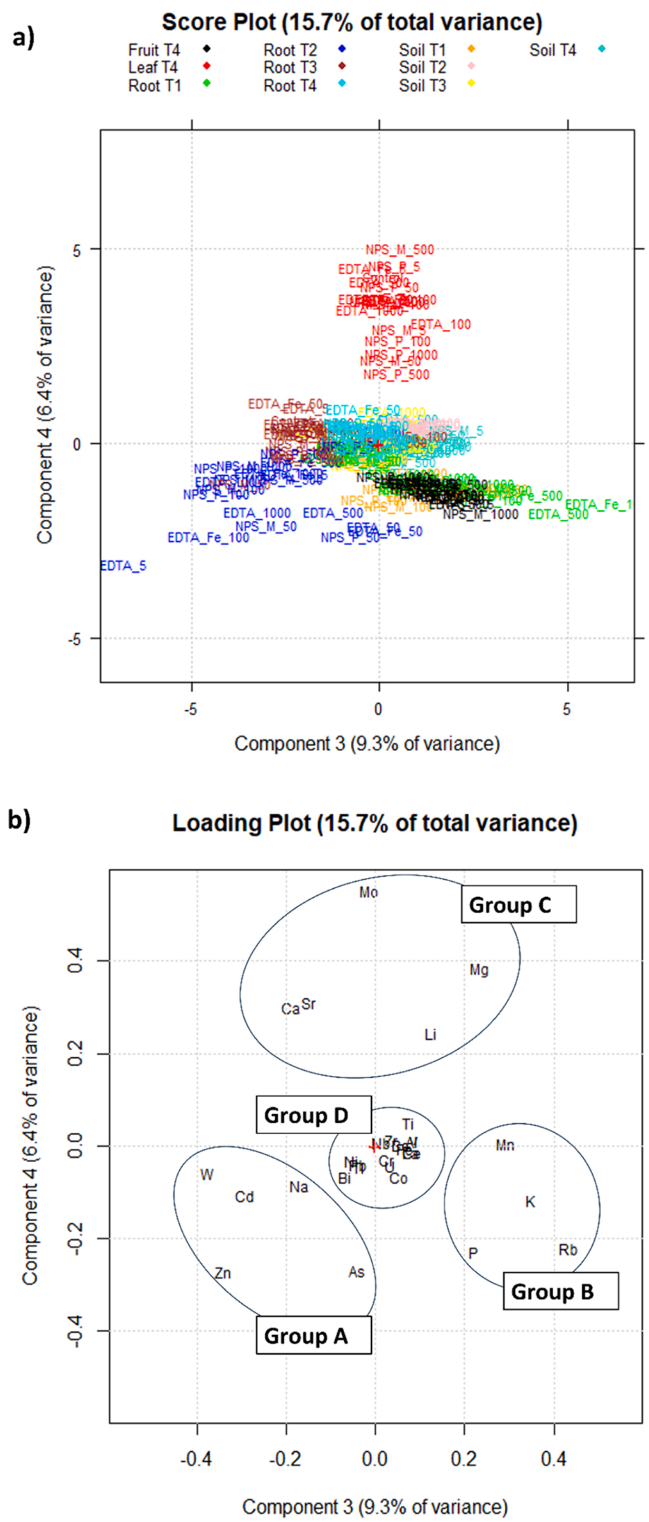

Fig. 4. Score (a) and loadings (b) plots of PC3/PC4 showing variability of element concentrations in all samples at all times of growth.

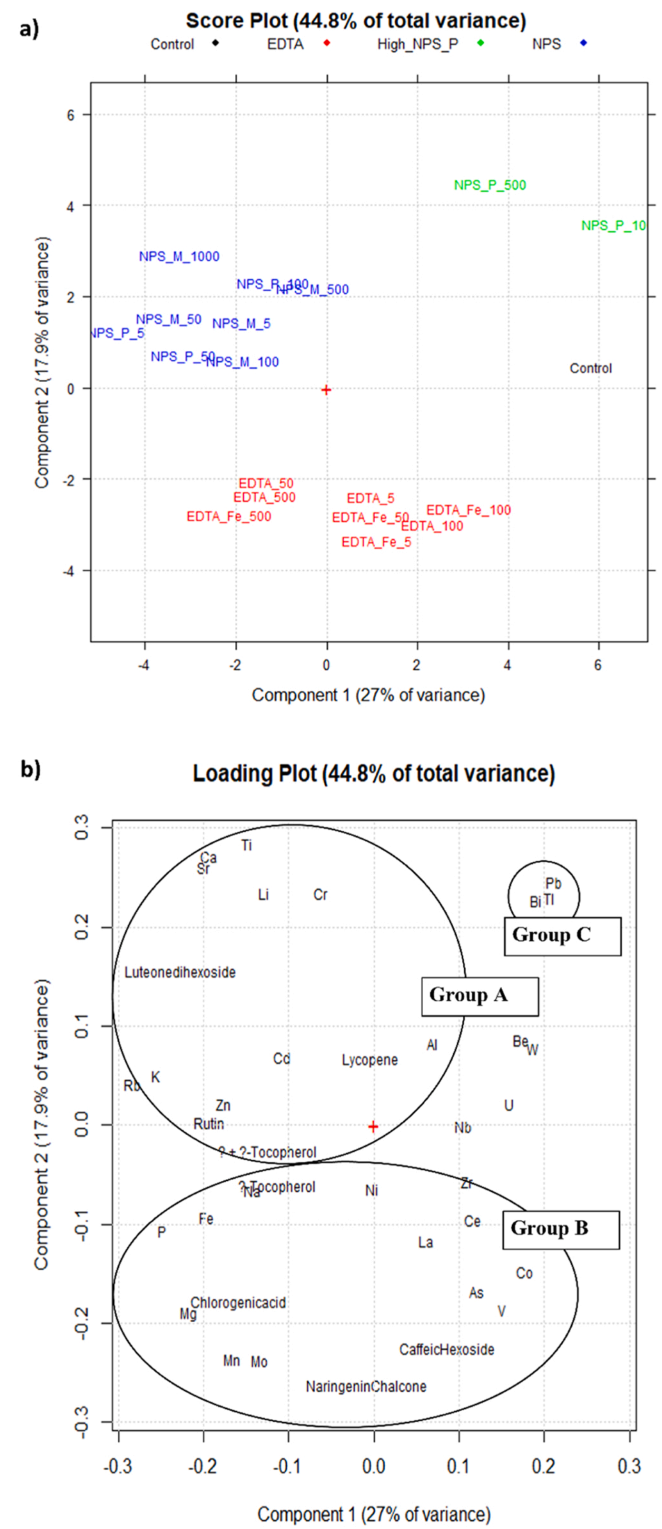

Fig. 5. Score and loading plots of PC1/PC2 showing variability of element concentrations and variability of phenolic compounds, carotenoids, and element concentrations in fruit samples (panel a and b) at T4.

showed, the main variability in the dataset (PC1) is explained by the different element concentrations in the leaf or fruit samples according to the different treatments they were subjected to. EDTA-based chelators at both low and high concentrations (5–1000 mg/L) increased translocation and accumulation in leaves of some elements (Figure S3a and S3b) including potentially toxic elements such as Cr, As and macronutrients such as K and P. On the other hand, NPs-based treatments increased translocation in the leaves of Ca, Co, Sr, Ti and V (Figure S3b, group A). Finally, high concentrations of EDTA (500 and 1000 mg/L) appeared to increase the translocation and accumulation of Bi, Fe, Na, Ni, Pb and Zn in the leaf organ.

Regarding the translocation and accumulation of the elements in the tomato fruits, the use of NPs- and EDTA-based chelators led to increased concentrations of macro- and micro-nutrients in fruits with respect to control (Fig. 5a and b). However, NPS- compared to EDTA-based treatments led to increased accumulation of some elements (Fig. 5b, group A) in fruits, including macro- and micro-nutrients such as Ca, K and Rb, while EDTA treatments led to increased concentrations of other elements (group B, Fig. 5b), including the nutrients Na, Mg and P. Finally, the highest concentrations of NPS-P (500 and 1000 mg/L) led to reduced accumulation of macro- and micro-nutrients in fruits while induced increased translocation and accumulation of Bi, Pb, and Tl (Figure S4). Interestingly, it can be seen that all treatments with NPs led to a large reduction in caffeic hexoside, chlorogenic acid and naringenin chalcone levels and to a considerable increase in lycopene, rutin, and luteone hexoside compared to treatments with EDTA and EDTA-Fe (Fig. 5b).

4. Discussion

The burgeoning field of plant nanotechnology offers promising avenues for enhancing crop yield and quality. While numerous studies have demonstrated that various nanoparticles (NPs) can improve plant physiological processes such as seed germination, photosynthesis, and metabolite synthesis (e.g., El-Saadony et al., 2022; El-Moneim et al., 2021; Singh et al., 2024), the specific impacts of iron phosphate ($FePO_4$) and magnetite (Fe_3O_4) nanoparticles on *Solanum lycopersicum* remain underexplored. This study uniquely investigates, for the first time, the comprehensive effects of $FePO_4$ and Fe_3O_4 NPs on tomato plants by combining detailed metabolic profiling of phenolic acids and carotenoids via LC-MS with an extensive ionomic analysis using ICP-MS.

In a novel contribution to this field, this study revealed that iron phosphate (NPS-P) and magnetite (NPS-M) nanoparticles significantly enhance *S. lycopersicum* growth, particularly at higher concentrations (100, 500, and 1000 mg/L). This enhancement was evident in increased plant biomass, altered soil pH, and higher leaf total chlorophyll and carotenoid content, outperforming both water controls and EDTA-Fe treatments. Conversely, high concentrations of EDTA-Fe (500 and 1000 mg/L) drastically reduced plant biomass and even inhibited the ripening stage, demonstrating its clear toxicity.

These findings align with existing literature showcasing the beneficial effects of magnetite nanoparticles on other plant species. For example, Zhu et al. (2008) observed that *Cucurbita maxima* accumulated Fe_3O_4 NPs without toxicity at 50 and 100 mg/L, though *Phaseolus limensis* showed no uptake, highlighting species-specific responses to nanoparticles. Similarly, Khater (2015) reported that foliar application of magnetite NPs (15 mg/L) boosted biomass and essential oil levels in *Mentha piperita L.*, increasing Mn, Zn, and Cu in various tissues. Tombuloglu et al. (2022) also found that magnetite NPs (100 and 200 mg/L) improved germination, biomass, and leaf pigmentation in barley (*Hordeum vulgare L.*), with increased tissue iron content indicating translocation without toxic effects. This consistent pattern across various studies supports the potential of iron-based nanoparticles as effective plant growth enhancers.

The observed increase in plant biomass with Fe_3O_4 (NPS-M) nanoparticles in our study aligns with previous research suggesting their role in promoting plant growth. This enhancement may stem from their ability to regulate phytohormone levels and antioxidant enzyme activity, which can effectively control reactive oxygen species (ROS) and thereby stimulate root development and overall plant growth (Rui et al., 2016). Recent proposals even suggest that magnetite-based nanofertilizers could entirely substitute conventional fertilizers like EDTA-Fe by boosting both plant biomass and antioxidant compounds (Garza-Alonso et al., 2023), exemplified by improved germination and seedling growth in *Quercus macdougallii* with magnetite NPs (750 mg/L).

While research on iron phosphate ($FePO_4$) nanoparticles is less extensive, our findings for NPS-P corroborate the limited existing literature. Sega, (2018), Sega et al. (2019, 2020) similarly reported that $FePO_4$ NPs enhanced root biomass and phosphorus content in hydroponically grown cucumber, and improved shoot growth and fresh biomass in maize, with iron accumulating primarily in the roots.

Conversely, our results unequivocally confirm the toxicity of EDTA-Fe, a common component in commercial fertilizers, particularly at higher concentrations. The application of EDTA-Fe significantly reduced growth and developmental parameters in our tomato plants, with severe toxicity at higher doses (500 and 1000 mg/L) even preventing flowering and fruiting. This toxicity was accompanied by decreased chlorophyll levels in leaves, likely due to iron chlorosis, which correlated with an increased soil pH that detrimentally altered Fe bioavailability and potentially facilitated heavy metal absorption, such as Lead (Pb).

Interestingly, NPS-M treatments resulted in slightly higher pH values than NPS-P at the same concentrations throughout plant growth. While both nanoparticle types induced an initial acidification of the soil, their long-term impact diverged. The treatment with NPS-M was able to induce a recovery of neutral soil pH compared to NPS-P at 50, 100 and 500 mg/L. According to our results, Zhang et al. (2020) found that the addition of ZnO-NPs and CuO-NPs caused significant increase in paddy soil pH, probably due to a $H+$ consumption by metal oxide nanoparticles.

This pH shift towards neutrality is primarily attributable to the soil natural buffering capacity, which actively works to counteract pH changes introduced by external factors. Beyond this inherent resilience, the recovery to neutrality can also be influenced by dynamic changes in nanoparticle surface chemistry as they transform in the soil, potentially altering their proton-donating or -consuming capabilities. Furthermore, shifts in microbial activity and community composition within the soil, potentially triggered by the nanoparticles, could lead to a net production of alkaline compounds or consumption of acidic ones over time. Lastly, plant-mediated effects, such as selective nutrient uptake patterns or the release of specific root exudates, can also play a role in modulating rhizosphere pH back towards neutrality (Zhang et al., 2024; Suazo--Hernández et al., 2023).

On the other hands, the observation that NPS-P induced beneficial soil acidification is a crucial aspect. First, the surface chemistry of the $FePO_4$ nanoparticles plays a fundamental role: their extremely high surface area can facilitate hydrolysis reactions that release hydrogen ions ($H+$) into the soil, thereby lowering the pH. Additionally, although generally considered stable, some degree of nanoparticle dissolution can release ions that, upon reacting with water, form acidic species. Second, as mentioned, nanoparticles can influence soil microbial activity. For example, they might stimulate microbial respiration, which produces carbon dioxide (CO2), and this, when dissolved in soil water, forms carbonic acid, lowering the pH. Finally, nanoparticles can interact directly with soil components, for instance, by affecting cation exchange or undergoing redox reactions that release protons (Suazo-Hernández et al., 2023). This capacity to acidify the soil is particularly advantageous because it can enhance the availability of essential nutrients that are less soluble at higher pH values, offering an innovative mechanism to optimize plant nutrition and reducing the need for traditional fertilizers that can lead to toxicity issues or soil alkalinization. The distinct behaviors observed between NPS-M and NPS-P highlight that the specific chemical properties and transformations of each nanoparticle type are crucial in determining their long-term impact on soil pH. Our findings regarding photosynthetic pigments are consistent with existing literature. Both NPS-M and NPS-P treatments significantly increased total chlorophyll and carotenoid levels in tomato leaves after the first month of treatment. This positive effect contrasts sharply with EDTA-Fe treatments at higher concentrations (500 and 1000 mg/L), which drastically reduced chlorophyll and carotenoid levels, leading to clear toxicity symptoms. The carotenoid and fat-soluble vitamin profiles in our control samples were consistent with those previously reported for tomato plants (Brasili et al., 2020). These pigment responses are intrinsically linked to soil pH dynamics. This study revealed that the addition of NPS-M and NPS-P slightly acidified the soil, a critical factor for nutrient availability. This stands in direct contrast to EDTA-Fe, which rendered the soil more alkaline (Baudoin et al., 2013). It is well-established that alkaline soil conditions reduce iron solubility and root absorption (Zuo and Zhang, 2011), thereby promoting the production of reactive oxygen species (ROS) and ultimately leading to iron chlorosis, a condition we observed with EDTA-Fe.

NPS-M and NPS-P at low concentrations (50 and 5 mg/L, respectively) significantly boosted phenolic compound levels. In particular the increase in phytoalexins such as chlorogenic acid and luteone hexoside can be attributed to the plants' stress response. On the other hands, an increase of these phenolic compounds was observed also as a defence response to EDTA and EDTA-Fe. Chlorogenic acid is one of the most abundant beneficial polypheols in plants and is well known as a nutritional antioxidant in plant-based foods. Apart from its dietary antioxidant activity, it has been proved to be an efficient defence molecule against a broad range of insect herbivores (Kundu et al., 2019) and as protecting molecules of plant tissues from damage by oxidative stress, pathogen infection, and wounds (Kim et al., 2019). Both chlorogenic acid and luteone hexoside possess strong antioxidant and anti-inflammatory properties (De Stefano et al., 2021; Wang et al., 2022). Our results indicate that by increasing their levels, tomato plants could enhance both the ability to scavenge the ROS generated due to the nanoparticle treatment and support the biosynthesis of protective secondary metabolites that contribute to the plant's resilience, by providing more precursors. The capacity of metal NPs to increase protective secondary metabolites was previously observed by Razavizadeh et al. (2024) showing that low levels of FeONPs (especially 200 mg l^{-1}) increased fresh weight (231 %), total chlorophyll (49 %), and total phenolics (259 %) content.

Furthermore, this study reveals distinct effects of EDTA- and NPs-based chelators on element dynamics and fruit quality in tomato plants. EDTA treatments enhanced the uptake and translocation of a broad range of elements, including potentially toxic ones, likely due to their strong chelating ability. Conversely, NPs, potentially due to their unique surface properties and interactions with soil components, appeared to exhibit more selectivity in their influence on element bioavailability. This selectivity is evident in the distinct set of elements (Ca, Co, Sr, Ti, V) whose translocation to leaves was promoted by NPs treatments. This suggests that NPs might be interacting with specific soil constituents or plant uptake mechanisms, leading to a more targeted effect on element mobilization compared to EDTA-based chelators. Strikingly, NPs treatments drastically altered fruit compound levels, decreasing certain phenolic compounds while increasing carotenoids, suggesting a significant impact on fruit metabolism, possibly through interactions with biosynthetic enzymes. The observed reduction in caffeic hexoside, chlorogenic acid and naringenin chalcone compared to EDTA-based treatments, alongside a substantial increase in Lycopene, Rutin, and Luteone hexoside suggests that NPs may be interacting with key enzymes involved in these biosynthetic pathways. This interaction could be direct, with NPs potentially binding to or modifying enzyme activity, or indirect, through NPs-induced changes in gene expression related to these enzymes. Surprisingly, high concentrations of NPS-P reduced fruit nutrient content alongside increased Bi, Pb, and Tl accumulation, potentially indicating a stress response. This stress could be interfering with nutrient uptake and translocation to the fruit, while simultaneously triggering the accumulation of other elements as a potential stress-coping mechanism. Surprisingly, as revealed by ICP-MS analysis, root Fe content did not exhibit a NPs concentration-dependent effect, suggesting that a sophisticated regulation of Fe uptake and transport is essential to maintain Fe homeostasis, prevent over-accumulation and toxicity phenomena (Kobayashi et al., 2012). Nanoaprticles can significantly alter the chemical environment in the rhizosphere, including reducing Fe (III) to more soluble Fe (II) or producing siderophores (Fe-chelating compounds), thus affecting iron availability to the plant (Riaz and Guerinot 2021). Indeed, iron solubility and speciation are highly pH dependent. At higher pH (as observed for NPS-M at longer times), Fe could precipitate as insoluble oxyhydroxides, reducing its bioavailability, even if there is a high Fe presence. Conversely, a decrease in pH might mobilize Fe. On the other hands, if nanoparticles cause fluctuating or non-linear pH changes across different concentrations, it could lead to inconsistent Fe availability. Furthermore, nanoparticles themselves can act as adsorbents, binding to soluble Fe ions or chelated Fe in the soil, thus forming stable complexes that are less available for root uptake. This complexation might not be linearly dependent on nanoparticle concentration, especially if binding sites become saturated or if nanoparticles aggregate, reducing their effective surface area. It should be also considered that roots release exudates that can alter the local rhizosphere environment. Nanoparticles might interact with these exudates, forming aggregates or coatings that could indirectly affect Fe uptake (Wang et al., 2025). These findings highlight the complex interplay between chelator type, element availability, and metabolic pathways, emphasizing the need for further research to understand the underlying mechanisms and optimize agricultural practices. The results of this study offer new insights into the response of tomato plants to Fe_3O_4 (NPS-M) and $FePO_4$ NPs (NPS-P) exposure and could be useful for designing alternative strategies to the use of commercial fertilizers.

5. Conclusions

This study provides compelling evidence for the potential of Fe_3O_4 (NPS-M) and $FePO_4$ (NPS-P) nanoparticles as innovative and sustainable alternatives to conventional fertilizers in tomato cultivation. Notably, this research, representing the first comprehensive investigation, to our knowledge, that simultaneously combined ionomic and metabolic profiling, revealed that these nanoparticles offer significant advantages over traditional chelators like EDTA-Fe, particularly in enhancing plant growth, photosynthetic efficiency, and the nutritional quality of tomato fruits. Our key findings highlighted that both NPS-M and NPS-P, especially at higher concentrations, significantly boosted plant biomass, total chlorophyll, and carotenoid levels in tomato leaves. This suggests an improved physiological performance and enhanced photosynthetic capacity in plants treated with nanoparticles. Crucially, NPS-P treatments beneficially acidified the soil, improving nutrient availability, a stark contrast to the observed toxicity and growth inhibition caused by high concentrations of EDTA-Fe. The detrimental effects of EDTA-Fe, including reduced biomass and inhibited ripening, underscore the need for more environmentally sustainable alternatives. Furthermore, the ionomic analysis revealed that nanoparticles exhibit a more selective influence on elemental bioavailability compared to the broad, and sometimes undesirable, uptake promoted by EDTA-based treatments. While EDTA broadly facilitated the uptake of various elements, including potentially toxic ones, nanoparticles specifically increased the accumulation of beneficial elements like Ca, Co, Sr, Ti, and V in leaves, and Ca, K, and Rb in fruits. This targeted elemental modulation suggests that nanoparticles could be tailored to address specific plant nutritional needs more efficiently. Beyond elemental uptake, the obtained results highlighted the significant impact of nanoparticles on fruit metabolism. We observed a notable increase in key health-promoting compounds such as chlorogenic acid and luteone hexoside in fruits treated with nanoparticles. This metabolic shift points towards the ability of nanoparticles to positively influence the nutritional profile of the harvested product. In conclusion, the application of iron-based nanoparticles (Fe_3O_4 (NPS-M) and $FePO_4$ (NPS-P)) presents a promising avenue for developing more sustainable and efficient agricultural practices. These findings not only contribute to the growing body of literature on agricultural nanotechnology but also offer a robust foundation for reducing reliance on commercial fertilizers. While our study illuminates the intricate interactions between nanoparticles, soil, and plant physiology, further research is essential to fully optimize nanoparticle application strategies. Future investigations should focus on elucidating the precise mechanisms underlying their selective elemental uptake and metabolic modulation, ultimately paving the way for their widespread and effective adoption in crop production.

CRediT authorship contribution statement

Gabriella Pasqua: Supervision. **Valerio Petruccelli:** Project administration, Methodology, Investigation. **Silvia Canepari:** Supervision. **Elisa Brasili:** Writing – review & editing, Writing – original draft, Validation, Supervision. **Emma Cocco:** Methodology, Formal analysis. **Lorenzo Massimi:** Writing – review & editing, Writing – original draft, Visualization, Validation, Data curation. **Emanuele Vaccarella:** Software, Methodology, Formal analysis. **Francesco Mura:** Methodology, Investigation, Funding acquisition. **Alessio Talone:** Formal analysis. **Domenico Rosa:** Investigation, Funding acquisition, Formal analysis. **Chiara Dal Bosco:** Formal analysis, Data curation. **Martina Iazzetta:** Formal analysis. **Luca Di Palma:** Supervision. **Alessandra Gentili:** Supervision.

Declaration of Competing Interest

The authors declare that they have no known competing financial interests or personal relationships that could have appeared to influence the work reported in this paper.

Appendix A. Supporting information

Supplementary data associated with this article can be found in the online version at doi:10.1016/j.plana.2025.100182.

Data availability

Data will be made available on request.

References

Abadía, J., Vázquez, S., Rellán-Álvarez, R., El-Jendoubi, H., Abadía, A., Álvarez-Fernández, A., et al., 2011. Towards a knowledge-based correction of iron chlorosis. Plant Physiol. Biochem 49, 471–482.

Ahmed, N., Zhang, B., Chachar, Z., Li, J., Xiao, G., Wang, Q., Tu, P., 2024. Micronutrients and their effects on horticultural crop quality, productivity and sustainability. Sci. Hortic. 323, 112512.

Arora, P.K., Tripathi, S., Omar, R.A., Chauhan, P., Sinhal, V.K., Singh, A., Singh, V.P., 2024. Next-generation fertilizers: the impact of bionanofertilizers on sustainable agriculture. Microb. Cell Factor. 23 (1), 254.

Baligar, V.C., Fageria, N.K., He, Z.L., 2001. Nutrient use efficiency in plants. Commun. Soil Sci. Plant Anal. 32, 921–950. https://doi.org/10.1081/CSS-100104098.

Barber, S.A., 1995. In: Barber, S.A. (Ed.), Soil Nutrient Bioavailability: a mechanistic approach. John Wiley, New York.

Baudoin, W., Nono-Womdim, R., Lutaladio, N., Hodder, A., Castilla, N., Leonardi, C., Duffy, R., 2013. Good agricultural practices for greenhouse vegetable crops: principles for Mediterranean climate areas. FAO.

Brasili, E., Bavasso, I., Petruccelli, V., Vilardi, G., Valletta, A., Dal Bosco, C., Di Palma, L., 2020. Remediation of hexavalent chromium contaminated water through zero-valent iron nanoparticles and effects on tomato plant growth performance. Sci. Rep. 10 (1), 1920.

Canepari, S., Pietrodangelo, A., Perrino, C., Astolfi, M.L., Marzo, M.L., 2009. Enhancement of source traceability of atmospheric PM by elemental chemical fractionation. Atmos. Environ. 43 (31), 4754–4765.

Cantu, J.M., Ye, Y., Hernandez-Viezcas, J.A., Zuverza-Mena, N., White, J.C., Gardea-Torresdey, J.L., 2022. Tomato fruit nutritional quality is altered by the foliar application of various metal oxide nanomaterials. Nanomaterials 12 (14), 2349.

Chhipa, H., 2017. Nanofertilizers and nanopesticides for agriculture. Environ. Chem. Lett. 15, 15–22.

Daszkiewicz, T., 2022. Food production in the context of global developmental challenges. Agriculture 12, 832.

De Stefano, A., Caporali, S., Di Daniele, N., Rovella, V., Cardillo, C., Schinzari, F., Terrinoni, A., 2021. Anti-inflammatory and proliferative properties of luteolin-7-O-glucoside. Int. J. Mol. Sci. 22 (3), 1321.

Dere, Ş., GÜNEŞ, T., Sivaci, R., 1998. Spectrophotometric determination of chlorophyll-A, b and totalcarotenoid contents of some algae species using different solvents. Turk. J. Bot. 22 (1), 13–18.

El-Moneim, D.A., Dawood, M.F., Moursi, Y.S., Farghaly, A.A., Afifi, M., Sallam, A., 2021. Positive and negative effects of nanoparticles on agricultural crops. Nanotechnol. Environ. Eng. 6 (2), 21.

El-Saadony, M.T., Saad, A.M., Soliman, S.M., Salem, H.M., Desoky, E.S.M., Babalghith, A. O., AbuQamar, S.F., 2022. Role of nanoparticles in enhancing crop tolerance to abiotic stress: a comprehensive review. Front. Plant Sci. 13, 946717.

Feng, Y., Kreslavski, V.D., Shmarev, A.N., Ivanov, A.A., Zharmukhamedov, S.K., Kosobryukhov, A., Shabala, S., 2022. Effects of iron oxide nanoparticles (Fe3O4) on growth, photosynthesis, antioxidant activity and distribution of mineral elements in wheat (Triticum aestivum) plants. Plants 11 (14), 1894.

Gamage, A., Gangahagedara, R., Subasinghe, S., Gamage, J., Guruge, C., Senaratne, S., Merah, O., 2024. Advancing sustainability: the impact of emerging technologies in agriculture. Curr. Plant Biol., 100420

Garza-Alonso, C.A., Cadenas-Pliego, G., Juárez-Maldonado, A., González-Fuentes, J.A., Tortella, G., Benavides-Mendoza, A., 2023. Fe2O3 nanoparticles can replace Fe-EDTA fertilizer and boost the productivity and quality of raphanus sativus in a soilless system. Sci. Hortic. 321, 112261.

Goyal, V., Rani, D., Ritika, Mehrotra, S., Deng, C., Wang, Y., 2023. Unlocking the potential of nano-enabled precision agriculture for efficient and sustainable farming. Plants 12, 3744.

Hawkesford, M., Horst, W., Kichey, T., Lambers, H., Schjoerring, J., Møller, I.S., , 2012. Chapter 6 - Functions of Macronutrients, in P. B. T.-M. M. N. of H. P. Ed. T. E. Marschner (San Diego: Academic Press), 135–189. doi: 101016/B978-0-12-384905-2.00006-6.

Hsieh, C.T., Chen, I.L., Chen, W.Y., Wang, J.P., 2012. Synthesis of iron phosphate powders by chemical precipitation route for high-power lithium iron phosphate cathodes. Electrochim. Acta 83, 202–208.

Iannilli, V., D'Onofrio, G., Marzi, D., Passatore, L., Pietrini, F., Massimi, L., Zacchini, M., 2024. Lithium toxicity in lepidium sativum L. Seedlings: exploring li accumulation's impact on germination, root growth, and DNA integrity. Environments 11 (5), 93.

Iannilli, V., Passatore, L., Carloni, S., Massimi, L., Giusto, C., Zacchini, M., Pietrini, F., 2025. Bismuth accumulation and toxicity in freshwater biota: a study on the bioindicator species lemna minor and echinogammarus veneris. Sci. Total Environ. 975, 179263.

Khater, M.S., 2015. Magnetite-nanoparticles effects on growth and essential oil of peppermint. Curr. Sci. Int. 4 (2), 140–144.

Kim, J.K., Park, S.U., 2019. Chlorogenic acid and its role in biological functions: an up to date. EXCLI J. 18, 310–316.

Kobayashi, T., Nishizawa, N.K., 2012. Iron uptake, translocation, and regulation in higher plants. Annu. Rev. Plant Biol. 63 (1), 131–152.

Kobayashi, T., Nozoye, T., Nishizawa, N.K., 2019. Iron transport and its regulation in plants. Free Radic. Biol. Med. 133, 11–20. https://doi.org/10.1016/j.freeradbiomed.2018.10.439.

Kundu, A., Vadassery, J., 2019. Chlorogenic acid-mediated chemical defence of plants against insect herbivores. Plant Biol. 21 (2), 185–189.

Lichtenthaler, H.K., Wellburn, A.R., 1983. Determ. Total carotenoids Chlorophylls a b leaf Extr. Differ. Solvents.

Mariyam, S., Upadhyay, S.K., Chakraborty, K., Verma, K.K., Duhan, J.S., Muneer, S., et al., 2023. Nanotechnology, a frontier in agricultural science, a novel approach in abiotic stress management and convergence with new age Medicine: a review. Sci. Total Environ., 169097

Priya, E., Sarkar, S., Maji, P.K., 2024. A review on slow-release fertilizer: nutrient release mechanism and agricultural sustainability. J. Environ. Chem. Eng., 113211

Razavizadeh, R., Anwari, A.A.S., Forghani, A.H., Mirmazloum, I., 2024. Application of iron oxide nanoparticles improves growth and phytochemical constituents of in vitro cultured carum copticum l. J. Agric. Food Res. 18, 101402.

Riaz, N., Guerinot, M.L., 2021. All together now: regulation of the iron deficiency response. J. Exp. Bot. 72 (6), 2045–2055.

Ribas-Agustí, A., Cáceres, R., Gratacós-Cubarsí, M., Sárraga, C., Castellari, M., 2012. A validated HPLC-DAD method for routine determination of ten phenolic compounds in tomato fruits. Food Anal. Methods 5 (5), 1137–1144.

Rosa, D., D'Agostino, F., Bavasso, I., Di Palma, L., 2023. An innovative and easy method for iron-doped titania synthesis. Chem. Eng. Trans. 101, 13–18.

Rui, M., Ma, C., Hao, Y., Guo, J., Rui, Y., Tang, X., Zhao, Q., Fan, X., Zhang, Z., Hou, T., Zhu, S., 2016. Iron oxide nanoparticles as a potential iron fertilizer for peanut (Arachis hypogaea). Front. Plant Sci. 7, 815.

Sánchez-Rodríguez, E., del Mar Rubio-Wilhelmi, M., Cervilla, L.M., Blasco, B., Rios, J.J., Leyva, R., Ruiz, J.M., 2010. Study of the ionome and uptake fluxes in cherry tomato plants under moderate water stress conditions. Plant Soil 335, 339–347.

Sega, Davide, 2018. FePO4 nanoparticles a source nutrients plants synthesis evaluation their effects hydroponically grown cucumber maize seedlings.

Sega, D., Baldan, B., Zamboni, A., Varanini, Z., 2020. FePO4 NPs are an efficient nutritional source for plants: combination of nano-material properties and metabolic responses to nutritional deficiencies. Front. Plant Sci. 11, 586470.

Sega, D., Ciuffreda, G., Mariotto, G., Baldan, B., Zamboni, A., Varanini, Z., 2019. FePO4 nanoparticles produced by an industrially scalable continuous-flow method are an available form of p and fe for cucumber and maize plants. Sci. Rep. 9 (1), 11252.

Selvakesavan, R.K., Kruszka, D., Shakya, P., Mondal, D., Franklin, G., 2023. Impact Nanomater. Plant Second. Metab. Nanomater. Interact. Plant Cell. Mech. Macromol. Agric. Implic. 133–170.

Singh, A., Agrawal, S., Rajput, V.D., Ghazaryan, K., Yesayan, A., Minkina, T., Alexiou, A., 2024. Nanoparticles in revolutionizing crop production and agriculture to address salinity stress challenges for a sustainable future. Discov. Appl. Sci. 6 (6), 317.

Singh, U.M., Sareen, P., Sengar, R.S., Kumar, A., 2013. Plant ionomics: a newer approach to study mineral transport and its regulation. Acta Physiol. Plant. 35, 2641-2653.22.

Suazo-Hernández, J., Arancibia-Miranda, N., Mlih, R., Cáceres-Jensen, L., Bolan, N., Mora, M.D.L.L., 2023. Impact on some soil physical and chemical properties caused by metal and metallic oxide engineered nanoparticles: a review. Nanomaterials 13 (3), 572.

Sun, X.D., Ma, J.Y., Feng, L.J., Duan, J.L., Xie, X.M., Zhang, X.H., Yuan, X.Z., 2023. Magnetite nanoparticle coating chemistry regulates root uptake pathways and iron chlorosis in plants. Proc. Natl. Acad. Sci. 120 (27), e2304306120.

Sun, Y., Zhu, G., Zhao, W., Jiang, Y., Wang, Q., Wang, Q., Gao, L., 2022. Engineered nanomaterials for improving the nutritional quality of agricultural products: a review. Nanomaterials 12 (23), 4219.

Tombuloglu, H., Albenayyan, N., Slimani, Y., Akhtar, S., Tombuloglu, G., Almessiere, M., Baykal, A., Ercan, I., Sabit, H., Manikandan, A., 2022. Fate and impact of maghemite (γ-Fe2O3) and magnetite (Fe3O4) nanoparticles in barley (Hordeum vulgare L.). Environ. Sci. Pollut. Res. 29 (3), 4710–4721.

Wang, D., Liu, Y., Tian, X., Guo, J., Luan, Y., Wang, D., 2025. Magnetite nanoparticle coating chemistry regulates root uptake pathways and iron chlorosis in plants. Proc. Natl. Acad. Sci. 122 (27), e2304306120.

Wang, L., Pan, X., Jiang, L., Chu, Y., Gao, S., Jiang, X., Peng, C., 2022. The biological activity mechanism of chlorogenic acid and its applications in food industry: a review. Front. Nutr. 9, 943911.

Watanabe, T., Maejima, E., Yoshimura, T., Urayama, M., Yamauchi, A., Owadano, M., Shinano, T., 2016. The ionomic study of vegetable crops. PLoS One 11 (8), e0160273.

Wu, H., Li, Z., 2022. Nano-enabled agriculture: how do nanoparticles cross barriers in plants? Plant Commun. 3 (6).

Xiao, L., Shibuya, T., Watanabe, T., Kato, K., Kanayama, Y., 2022. Effect of light quality on metabolomic, ionomic, and transcriptomic profiles in tomato fruit. Int. J. Mol. Sci. 23 (21), 13288.

Zacchini, M., Gullotta, G., D'Onofrio, G., Bertolotto, P., Massimi, L., Pietrini, F., 2023. Effects of lithium on morpho-physiological and ionomic traits in cannabis sativa L. Microshoots under in vitro conditions. Plant Cell Tissue Organ Culture (PCTOC 155 (3), 873–882.

Zhang, W., Long, J., Li, J., Zhang, M., Ye, X., Chang, W., Zeng, H., 2020. Effect of metal oxide nanoparticles on the chemical speciation of heavy metals and micronutrient bioavailability in paddy soil. Int. J. Environ. Res. Public Health 17 (7), 2482.

Zhang, X., Zhang, D., Sun, W., Wang, T., 2019. The adaptive mechanism of plants to iron deficiency via iron uptake, transport, and homeostasis. Int. J. Mol. Sci. 20, 2424. https://doi.org/10.3390/ijms20102424.

Zhang, H., Zheng, T., Wang, Y., Li, T., Chi, Q., 2024. Multifaceted impacts of nanoparticles on plant nutrient absorption and soil microbial communities. Front. Plant Sci. 15, 1497006.

Zhu, H., Han, J., Xiao, J.Q., Jin, Y., 2008. Uptake, translocation, and accumulation of manufactured iron oxide nanoparticles by pumpkin plants. J. Environ. Monit. 10 (6), 713–717.

Zuo, Y., Zhang, F., 2011. Soil and crop management strategies to prevent iron deficiency in crops. Plant Soil 339, 83–95.

Further reading

Zhou, D.M., Jin, S.Y., Wang, Y.J., Wang, P., Weng, N.Y., Wang, Y., 2012. Assessing the impact of iron-based nanoparticles on ph, dissolved organic carbon, and nutrient availability in soils. Soil Sediment Contam. Int. J. 21 (1), 101–114.